# Dynamic Nuclear Polarization Studies of Labile Complex Formation between Lithium Ion and Nitronyl Nitroxide or Imidazoline-1-oxyl Radical Ligands[1a]

**B. E. Wagner,* [1b] J. W. Linowski,[1b,c] J. A. Potenza,[1b] R. D. Bates, Jr.,[1d] J. N. Helbert,[1e] and E. H. Poindexter[1e]**

*Contribution from School of Chemistry, Rutgers University, New Brunswick, New Jersey 08903, Department of Chemistry, Georgetown University, Washington, D.C. 20057, and U.S. Army Electronics Technology and Devices Laboratory (ECOM), Fort Monmouth, New Jersey 07703.* *Received September 24, 1975*

**Abstract:** Transient complexation has been observed in alcoholic solutions of lithium ions and nitronyl nitroxide or imidazoline-1-oxyl free radicals (R-Y) chosen to provide a range of complexation abilities (R = 2-pyridyl (Py), 6-bromo-2-pyridyl (BrPy), phenyl (Ph), or 3-bromophenyl (BrPh); radical Y = nitronyl nitroxide (NO) or imidazoline-1-oxyl (IN)). In EtOH solutions, $^7$Li DNP enhancements and relaxation rates depend strongly upon the substituent R and reflect considerable rotational modulation (arising from complexation) of the spin-spin interaction. Detailed analysis indicates that labile $Li^+ \ldots$ R-Y complex formation occurs at sites preferred in the analogous protonation reactions. Calculated complex lifetimes vary from $2.5 \times 10^{-9}$ s for the weakly coordinating, monodentate BrPhNO ligand to $1.3 \times 10^{-8}$ s for the chelating ligand PyNO. Despite the short complex lifetimes, geometries similar to those found for stable complexes and $Li^+ \ldots$ R-Y approach distances near the sum of van der Waals radii are required to interpret the relaxation data. Both PyNO and PyIN appear to form respective N,O and N,N chelated adducts, while blockage of the Py coordination site in the BrPy derivatives yields $^7$Li enhancement and relaxation data similar to that of monodentate Ph derivatives. Because of their short correlation times, none of the above interactions was observable by ESR. In MeOH, much smaller differences in $^7$Li enhancement and relaxation parameters are observed. For all ligands, dipolar relaxation rates and derived complex lifetimes are substantially smaller than those in EtOH, indicating weaker $Li^+ \ldots$ R-Y complexation in the more polar medium. Blockage of the diimine coordination site in PyIN by the addition of $Hg^{2+}$ changes the solution ESR spectrum to that of the known $HgPyIN^{2+}$ complex and causes the $^7$Li enhancement and relaxation to revert to values indicative of fast, diffusion-controlled, outer-sphere collisions of $Li^+$ with the radical-Hg complex.

The development of sensitive spectroscopic techniques has led to increasingly more sophisticated insights into the subtleties of reaction mechanisms and the dynamics of molecular interactions in solution. While NMR and ESR techniques provide powerful probes for the study of dynamic interactions slower than about $10^{-8}$ s, the faster range to the diffusion limit of $10^{-11}$ s is much less accessible. This $10^{-8}$-$10^{-11}$ s range encompasses the chemically important time scale of molecular collisions in solution.

Intermolecular dynamic nuclear polarization (DNP) is responsive to molecular encounters over precisely this range of fast interaction times.[2,3] When supplemented by ESR and low-field nuclear spin-lattice relaxation measurements, collision parameters such as sticking times and radical-nucleus distances of closest approach may be determined from DNP measurements at one magnetic field.[4,5]

We have shown how DNP can monitor the interaction of ligands or solvent molecules with the surface of stable paramagnetic metal complexes (second coordination sphere interaction).[5a] The present study extends the applicability of DNP to the opposite limit, where the interaction of a metal ion with a radical ligand is highly transitory. Recently, we reported DNP results for $^7$Li ions in solutions containing the organic radical ions tetrachlorosemiquinone ($TCSQ^-$), tetracyanoethylene ($TCNE^-$), tetracyanoquinodimethane ($TCNQ^-$), and tetramethylphenylenediamine ($WBPC^+$).[5b] Although radical ESR spectra remained essentially unchanged upon addition of $^7$Li ($I = 3/2$) cations to these solutions, $^7$Li dipolar relaxation rates varied over a wide range. For all radical ions, $^7$Li DNP enhancements were negative, indicating the dominance of dipolar coupling. The seemingly weak scalar coupling, however, was often deceptive; although it reflected the absence of complexation interactions for $WBPC^+$, it was due to long complex lifetimes ($\tau_c \geq 10^{-8}$ s) for the anions.

In the present study, we examine the interaction of $Li^+$ ions with neutral radical nitronyl nitroxide[6] and imidazoline-1-oxyl[7] ligands of graduated complexation abilities.[8] As seen from ESR spectra changes, these ligands form either stable, labile, or no radical complexes with metal ions,[8] and are thus likely to provide a graded series of transient adducts with $Li^+$. The derived interaction times, distances of closest approach, adduct geometries, and induced spin densities at lithium should more fully characterize the molecular dynamics of labile complexation.

An electronics application interest in these systems lies in the need for spin-label molecules responsive to alkali metal and hydroxyl impurities on materials surfaces (for example, $SiO_2$).[9] An assortment of labels with diverse and well-characterized complexation properties is an essential basis for such studies. In another scientific area, the behavior of $Li^+$ in the vicinity of imidazoline-type bases may be of value in the study of the transport and mobility of alkali metal ions in biological systems.

## Theory

The theory governing nuclear relaxation and dynamic polarization of spin $3/2$ nuclei has been developed in terms of scalar ($c$) and dipolar ($q$, $r$, $s$) relaxation transition probabilities connecting spin states of the Zeeman Hamiltonian (Figure 1).[10] The spin-lattice relaxation rate ($T_{1n}^{-1}$) in the radical-containing solution is given by:

$$T_{1n}^{-1} = R_{1n} = R_d + R_c + R_b = R_p + R_b \qquad (1)$$

Here, $R_b$ is the bulk nuclear rate in the absence of radical species, $R_d$ is the dipolar rate induced by the radical, and $R_c$ is the scalar rate. The total radical-induced rate is $R_p$.

Dipolar relaxation can be modulated either by translational diffusion between the electron and nuclear species or by rotation of a transient radical-receptor complex. For translational diffusion, the dipolar relaxation rate is given by:

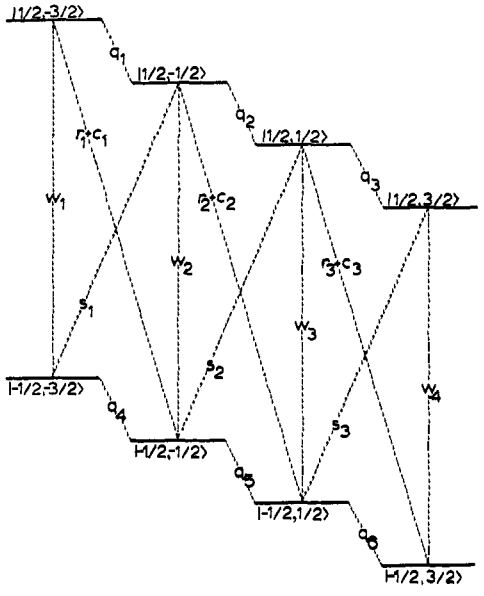


**Figure 1.** Spin states and relaxation transitions for an electron coupled to a nucleus of spin ½.

$$R_{dt} = \frac{2}{5}\pi\gamma_e^2\gamma_n^2h^2\tau_t d_t^{-3}N_e\left[\mathcal{J}_t(q) + \frac{7}{3}\mathcal{J}_t(r,s)\right] \quad (2)$$

where

$$\tau_t = 6\pi a\eta d_t^2/5kT \quad (3)$$

In eq 2 and 3, $N_e$ is the unpaired electron concentration (spins/cm$^3$), $\tau_t$ is the translational correlation time, $\mathcal{J}_t$ is the translational spectral density function, $d_t$ is the radical-receptor distance of closest approach, $a$ is the radius of the interacting particles, and $\eta$ is solution viscosity. For solutions of concern here, $\mathcal{J}_t$ approaches unity in the low-field limit. Thus one obtains

$$R_{dt} = 8\pi^2\gamma_e^2\gamma_n^2h^2a\eta d_t^{-1}N_e/5kT \quad (4)$$

For the case $d_t = 2a$ (particles of equal size), eq 4 reduces to that given by Abragam for the spin ½ case.[11] If the radical radius $a_1$ and the spin receptor radius $a_2$ are very different, $2a_1a_2/(a_1 + a_2)$ should be substituted for $a$ in eq 3 and 4.

For rotational modulation of the dipolar coupling, the corresponding expressions are

$$R_{dr} = \frac{3}{10}\gamma_e^2\gamma_n^2\hbar^2\tau_r d_r^{-6}(N_B/N_T) \times\left[\mathcal{J}_r(q) + \frac{7}{3}\mathcal{J}_r(r,s)\right] \quad (5)$$

where

$$\tau_r = 4\pi b^3\eta/3kT \quad (6)$$

Here, $\tau_r$ is the rotational correlation time, $\mathcal{J}_r$ is the rotational spectral density function, $N_B$ is the number of lithium ions bound to all radical molecules, $N_T$ is the total number of lithium ions in solution, $d_r$ is the average pair radius of the rotating adduct, and $b$ the effective tumbling radius of the molecular complex. In eq 5, the fraction $N_B/N_T$ contains the radical concentration implicitly. The terms $\mathcal{J}_r$ approach unity. Simplification yields:

$$R_{dr} = 4\pi\gamma_e^2\gamma_n^2h^2b^3\eta d_r^{-6}(N_B/N_T)/3kT \quad (7)$$

It will be helpful to consider dipolar relaxation rates expected theoretically for the two collision models. For EtOH solutions, with a radical-$Li^+$ complex volume $4\pi b^3/3 = 120 \times 10^{-24}$ cm$^3$, two values of partitioning complex formation $N_B/N_T = 1/1$ and $1/28$ (mole ratios of Li vs. EtOH in 1 M lithium salt solutions) and a distance of closest approach $d_r = 2.1$ Å and $d_t = 3.76$ Å, the following ranges for $^7$Li relaxation rates per mole of radical are determined: translational diffusion $R_{dt} = 80$ s$^{-1}$ M$^{-1}$; moderate complexation $N_B/N_T = 1/28$, $R_{dr} = 1400$ s$^{-1}$ M$^{-1}$; and maximum complexation $N_B/N_T = 1/1$, $R_{dr} = 39\,000$ s$^{-1}$ M$^{-1}$. For Li-MeOH solutions, the corresponding rates are: translational diffusion, $R_{dt} = 27$ s$^{-1}$ M$^{-1}$; moderate complexation $N_B/N_T = 1/40$, $R_{dr} = 330$ s$^{-1}$ M$^{-1}$; strong complexation $N_B/N_T = 1/1$, $R_{dr} = 13\,000$ s$^{-1}$ M$^{-1}$. Dipolar relaxation is seen to increase sharply with increasing complexation.

Approach distances used above for the diffusional interaction are derived from molecular weight and solution density. The sticking distance $d_r$ has been taken as the Li-N van der Waals sum of 2.1 Å.

Scalar spin-spin interactions are modulated by time-dependent changes in spin density at the receptor nucleus. The scalar relaxation rate $R_c$ is given as:

$$R_c = \frac{1}{2}\mathcal{A}^2\tau_c(N_B/N_t)\mathcal{J}_c(c) \quad (8)$$

where

$$\mathcal{J}_c(c) = [1 + (\omega_e + \omega_n)^2\tau_c^2]^{-1} \approx [1 + \omega_e^2\tau_c^2]^{-1} \quad (9)$$

The scalar correlation time $\tau_c$ is usually the complex lifetime, while $\mathcal{A}$, the isotropic hyperfine coupling constant in angular frequency units, is a measure of the induced spin density. Electron-electron exchange can influence the apparent sticking time

$$\tau_c^{-1} = \tau_{exch}^{-1} + \tau_{stick}^{-1} \quad (10)$$

The exchange rate, which increases with radical concentration, may be gauged from the presence and sharpness of intramolecular radical hyperfine structure. A fully resolved spectrum requires (approximately)[12]

$$\tau_{exch} \geq 10\mathcal{A}_{intra}^{-1} \quad (11)$$

The NMR enhancement, obtained by saturating ESR transitions, may be used to separate scalar and dipolar relaxation rates. In the limit of extreme motional narrowing, the ultimate enhancement $U_\infty$ (extrapolated from the directly observed enhancement $G$) is given by:

$$U_\infty = |(\gamma_e/\gamma_n)|(R_c - \tfrac{1}{2}R_d)/(R_c + R_d) \quad (12)$$

For purely dipolar interactions ($R_c = 0$), one obtains $U_\infty = -\frac{1}{2}|\gamma_e/\gamma_n|$, while for predominating scalar coupling $R_c \gg R_d$, one obtains $U_\infty = |\gamma_e/\gamma_n|$.

The absence of observable hyperfine coupling from $^7$Li in the ESR solution spectra provides an upper limit for $\tau_c$ from the relation:[12]

$$\tau_c \leq (5\mathcal{A})^{-1} \quad (13)$$

which yields $\tau_c \leq 1 \times 10^{-8}$ s for $\mathcal{A} = 1$ G or 2.8 MHz. The assumption of rotational dipolar modulation establishes a lower limit for $\tau_c$, which must be no less than $\tau_r$.

Fully determined correlation times require multifield observations to reveal the decline in relaxation rates as the various Larmor frequencies exceed the upper limits of the motional spectrum. In the absence of such extensive data, a simple estimation technique is adopted here. The sticking time is derived from the excess of observed relaxation rate over the expected translational rate, which arises from the rotational contribution of the transient complex, and yields $N_B/N_T$. The sticking time may be approximated on the principle that, to first order, the bound mole fraction is proportional to the sticking time, i.e.,

$$\tau_c = \tau_t(N_B/N_T)/(N_{B0}/N_T) \quad (14)$$

**Table I.** DNP Parameters for R-Y Radical Ligands in EtOH Solutions[a]

| Radical | $G_H$[b] | $G_{Li}$[b] | $U_{\infty Li}$ | $R_{pH}$[c] | $R_{pLi}$[c] | $R_{dLi}$[c] | $R_{cLi}$[c] |
|---|---|---|---|---|---|---|---|
| PyNO | −29 | −43 | −425 | 550 | 7380 | 6150 | 1230 |
| BrPyNO | −46 | 69 | 500 | 400 | 1700 | 800 | 900 |
| PhNO | −54 | 97 | 600 | 450 | 930 | 400 | 530 |
| BrPhNO | −36 | 99 | 850 | 450 | 960 | 320 | 640 |
| PyIN | −65 | −107 | −550 | 300 | 1260 | 1120 | 140 |
| BrPyIN | −67 | −50 | −260 | 330 | | | |
| PhIN | −69 | −58 | −260 | 290 | | | |
| BrPhIN | −58 | −67 | −380 | 350 | | | |
| PhIN[d] | −62 | −50 | −280 | 290 | | | |

[a] 1 M LiBr except where indicated. [b] Enhancement at 40 W applied ESR power. $U_{\infty H} = -330$ in all cases. [c] In $s^{-1}$ $mol^{-1}$. [d] 1 M LiCl solution.

The translational correlation time $\tau_t$ is the occupancy time at the complexation site in the absence of sticking; $N_{BO}/N_T$ is the mole fraction in the complexation site for freely diffusing molecules, and is simply the ratio of site volume to total volume.

## Experimental Procedures

Eight free radicals, shown in Figure 2, were studied; these were prepared by following published methods.[6-8] The radical solutions, when deoxygenated, were stable for weeks. Radical concentrations ranged from $5 \times 10^{-4}$ to $2 \times 10^{-1}$ M. Both high and low radical concentrations were needed to reveal and correct any unwanted effects due to electron spin exchange, and to optimize instrumental parameters for DNP and relaxation measurements.

DNP measurements were made at 70 G and ambient temperature (22 ± 2 °C) using instruments and techniques described elsewhere.[13] ESR data were obtained using a Varian 4500 spectrometer equipped with a dual cavity. Spin-lattice relaxation times were measured by the spin-echo method at 3700 G for bulk samples, and by growth and decay of the enhanced signal at 70 G for radical-containing samples. Samples were deoxygenated by five freeze-pump-thaw cycles and sealed in glass under vacuum. For DNP measurements, the sample size was 6 ml. Except where noted, $^7Li$ was present as 1 M in LiCl for methanol solutions and 1 M in LiBr for ethanol solutions. (Previous investigations have shown that variation of counterion has scant effect on DNP results.) Using a calibrated Ostwald viscometer, the viscosities of these solutions were found to be 0.01 and 0.03 P, respectively.

All $^1H$ (298 kHz) and $^7Li$ (115.6 kHz) enhanced signals were measured directly (ESR frequency 210.7 MHz), while time averaging of unenhanced NMR signals was necessary. A total of 6000 to 8000 traces of 5 s each with a digital signal averager was required to give $U_{\infty Li}$ values to a precision of ±20% for LiCl/MeOH solutions, while LiBr/EtOH solutions required up to 40 000 traces to achieve the same signal-to-noise ratio.

Among the R-IN ligands, $^7Li$ relaxation rates could be determined only for PyIN, due to low signal enhancements in the required dilute radical solutions. In contrast, good unenhanced proton signals were obtained after 16-32 traces. In most instances ultimate enhancements were determined by extrapolation to infinite applied rf power, followed by correction for leakage. However, some were determined by the ratio method.[14]

## Results and Discussion

**General Features.** NMR signal enhancements, radical-induced relaxation rates, and ultimate enhancements are shown in Table I for 1 M LiBr/EtOH solutions and in Table II for 1 M LiCl/MeOH solutions. Proton enhancements extrapolate to the dipolar limit and are not reported. Proton relaxation rates vary by at most a factor of two when radical and solvent are varied. In general, radical-induced proton rates for R-NO derivatives are slightly larger than for R-IN derivatives, while relaxation rates in ethanol solutions tend to be larger than those in methanol.

In contrast to the proton results, $^7Li$ relaxation rates vary by two orders of magnitude. For a given radical, lithium relaxation rates in ethanol are significantly larger than those in the corresponding methanol solution. In EtOH, there is overall

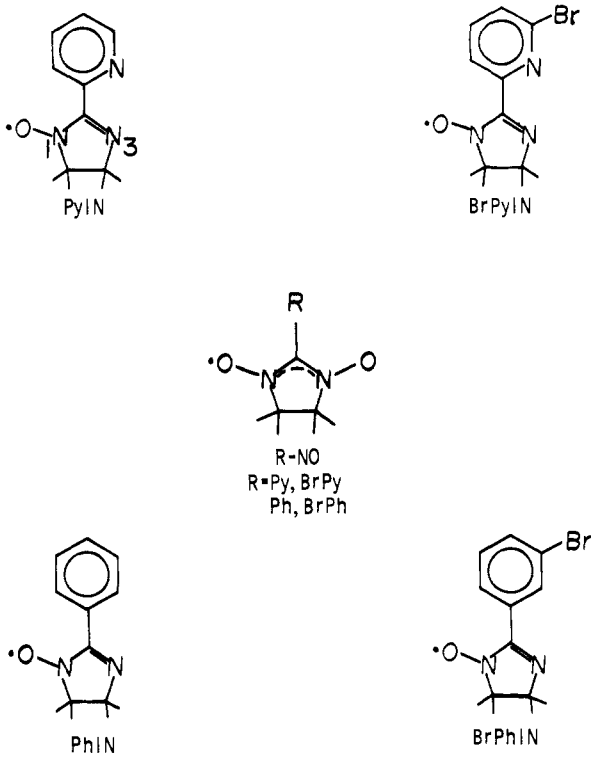


**Figure 2.** Nitronyl nitroxide and imidazoline-1-oxyl radicals used in this study.

a very large variation in both enhancement and relaxation rate; there is less variation in the MeOH series. In LiBr/EtOH solutions, observed dipolar relaxation rates lie within the range expected for fairly weak to fairly strong complexation, and cannot arise from translational diffusion alone.

In LiCl/MeOH solutions, observed rates indicate that dipolar modulation in MeOH is primarily translational and only weak transient complexes are formed. These results may be compared with $R_{dLi}$ values obtained for radical ions in MeOH. With the radical cation Wurster's blue, $R_{dLi}$ was found to be 18 $s^{-1}$ $M^{-1}$, corresponding to pure translational modulation, while for the radical anion tetrachlorosemiquinone, $R_{dLi}$ was 860 $s^{-1}$ $M^{-1}$, corresponding to moderately strong complexation.

The ESR spectra of many nitronyl nitroxide and imidazoline solutions have been described previously.[8b] The radical nitrogen hyperfine structure is fully resolved at radical concentrations used for relaxation rate measurements. Maximum exchange rates are thus determined: for PyNO ($\mathcal{A}_N = 8$ G), $\tau_{exch} \geq 7 \times 10^{-8}$ s; for PyIN($\mathcal{A}_N = 4$ G), $\tau_{exch} \geq 1.4 \times 10^{-7}$ s. No $^7Li$ intermolecular hyperfine structure was observed in any sample.

**Complex Lifetimes and Hyperfine Coupling Constants.** The

**Table II.** DNP Parameters for R-Y Radical Ligands in MeOH Solutions[a]

| Radical | $G_H$[b] | $G_{Li}$[b] | $U_{\infty Li}$ | $R_{pH}$[c] | $R_{pLi}$[c] | $R_{dLi}$[c] | $R_{cLi}$[c] |
|---|---|---|---|---|---|---|---|
| PyNO | −82 | 316 | 1100 | 340 | 625 | 145 | 480 |
| BrPyNO | −95 | 510 | 1500 | 390 | 650 | 50 | 600 |
| PhNO | −79 | 304 | 1275 | 322 | 470 | 80 | 390 |
| BrPhNO | −68 | 314 | 1400 | 360 | 330 | 40 | 290 |
| PyIN | −119 | 280 | 760 | 270 | 240 | 90 | 150 |
| BrPyIN | −100 | 144 | 500 | | | | |
| PhIN | −57 | −39 | −250 | | | | |
| BrPhIN | −86 | −70 | −300 | | | | |
| PyIN[d] | −143 | 330 | 1000 | 330 | 370 | 100 | 270 |
| $HgPyIN^{2+}$ [d] | −50 | −127 | −815 | 300 | 40 | 40 | 0 |

[a] 1 M LiCl except where indicated. [b] Enhancement at 40 W applied ESR power. $U_{\infty H} = -330$ in all cases. [c] In $s^{-1}$ $mol^{-1}$. [d] 1 M $LiNO_3$ solution.

**Table III.** Calculated Sticking Times, Approach Distances, and Hyperfine Coupling Constants of $^7Li$ Ions in Free-Radical Solutions

| Sample System | $\tau_c$, $10^{-11}$ s | $d_r$, Å | $\mathcal{A}$, G |
|---|---|---|---|
| | EtOH | | |
| PyNO | 1300 | 2.2 | 0.9 |
| BrPyNO | 430 | 2.7 | 0.8 |
| PhNO | 320 | 2.8 | 0.5 |
| BrPhNO | 250 | 2.9 | 0.7 |
| PyIN | 450 | 2.7 | 0.25 |
| | MeOH | | |
| PyNO | 43 | 2.2 | 0.9 |
| BrPyNO, PhNO, BrPhNO (av) | 48 | 2.8 | 0.9 |
| PyIN | 66 | 2.7 | 0.35 |

absence of $^7Li$ hyperfine structure establishes an upper bound for $\tau_c$, which, together with the diffusional lower bound, enables calculation of sticking times (Table III). The sticking times are all substantially smaller than the exchange times, and thus dominate nuclear relaxation. Sticking time varies over a range of 1:30 from weakly complexed NO ligands in MeOH to strongly complexed Li-PyNO in EtOH. For a given radical, $\tau_c$ is longer in EtOH than in MeOH. In LiCl/MeOH, relatively little change in sticking time is observed upon change of radical. A much larger range of sticking times is observed for the LiBr/EtOH solutions.

Hyperfine coupling energies are also listed in Table III for those cases where precision of the data warrants a calculation. The intermolecular $\mathcal{A}$ values, ranging from 0.25 to 0.9 G, are comparable to those observed in more firmly bound systems, such as the lithium-glyoxal bis(*N-tert*-butylimine) adduct (Li-GLIR) discussed below.

The reasonable assumption that hyperfine energy varies somewhat with distance of approach (although no useful exact relation is known) imposes enough additional constraints to enable a rough calculation of $d_r$ values. These are included in Table III. The interaction of $Li^+$ with R-NO and R-IN ligands endures at most 600 times as long as the time associated with translational diffusion ($\tau_{tLi}$ ca. $2 \times 10^{-11}$ s). Nevertheless, the transient adducts already exhibit bond distances that would be predicted for more stable complexes.

The results indicate that the ability of R-NO and R-IN ligands to coordinate to $Li^+$ ions depends strongly upon both the medium and the structure of the ligand itself. To interpret these results meaningfully, we should first consider some general properties of the radicals as ligands, and of $Li^+$ as a coordinating metal.

**Properties of the Ligands.** Interactions of metal ions with R-IN radicals that produce significant scalar coupling may take place by collisions with either the nitroxide oxygen atom or the N(3) imine atom. With the R-NO radicals, only the N-O groups contain appreciable spin density, and so collisions producing large spin density at $Li^+$ directly must occur at these sites. In addition, complexation with both R-IN and R-NO ligands may first occur at spin-remote sites, and conformational changes may then bring $Li^+$ close enough to the radical site to produce spin polarization.

The spin density distribution in R-IN radicals differs significantly from that in R-NO radicals. In the imidazoline-1-oxyl ligands, unpaired electron density is distributed unequally between the nitroxide and imidazole groups, and is concentrated on the former. Typical values for the hyperfine coupling constants and implied spin densities are:[7,8] for NO groups, $\mathcal{A}_{N1} = 9.2$ G, $\rho_{N1}^{\pi} = 0.38$, $\rho_O^{\pi} = 0.41$; for IN groups, $\mathcal{A}_{N3} = 4.3$ G, $\rho_{N3}^{\pi} = 0.16$. With R-NO ligands, equal spin density occurs at both nitrogens, $\mathcal{A}_N = 8$ G, $\rho_N^{\pi} = 0.3$, $\rho_O^{\pi} = 0.13$,[6,15] and is approximately a factor of two smaller than typically found for dialkyl nitroxides, $\mathcal{A}_N = 14$-16 G, $\rho_N^{\pi} = 0.6$-0.7, $\rho_O^{\pi} = 0.4$-0.3.[16]

The ligands differ in their relative ability to be protonated and to complex with various metals.[8] The nitronyl nitroxide group can be monoprotonated at a nitroxide oxygen atom in $CF_3COOH$, while the imidazoline-1-oxyl group in similar solutions is monoprotonated at the N(3) imine site only. As seen by ESR spectroscopy, R-NO ligands do not form metal complexes at the paramagnetic sites, while R-IN ligands interact at the N(3) sites to form complexes that are long-lived on the ESR time scale ($\tau_c > 1 \times 10^{-7}$ s).

Substituents modify protonation and complexation interactions at the radical site. The 2-pyridyl ligand PyNO is protonated exclusively at the essentially diamagnetic pyridine nitrogen site,[8,17] while PyIN undergoes double protonation, with protonation at the pyridine nitrogen occurring first. Blockage of the pyridyl coordination site in BrPyNO and BrPyIN changes the behavior of these ligands to that of the corresponding phenyl and bromophenyl derivatives.

**Lithium Coordination Properties.** Solid-state complexes between $Li^+$ and pyridine or ethylenediamine show distances close to the sum of the van der Waals radii (ca. 2.1 Å).[18] The structures of PhNO[19] and various pyridyl imine ligands[20] make it clear that coordination of $Li^+$ to PyNO could occur via chelation with the pyridyl nitrogen and a nitronyl oxygen atom, while coordination to PyIN could occur through both pyridyl and imidazoline imine nitrogen atoms.

In solution, several chelated $Li^+$ adducts have been observed by ESR with basic ligands analogous to PyIN. For example, the GLIR radical anion interacts[21] with $Li^+$ to give an $\alpha$-diimine chelated adduct with $\mathcal{A}_{Li} = 1.3$ G in DME. Indeed, this complex is so strong that in a solution of Li-GLIR, no free ligand was detected. Similarly, the 2,2′-bipyridyl radical anion

yields a Li adduct with $\mathcal{A}_{Li} = 0.7$ G in the same solvent.[22]

**Structures of the Transient Complexes. LiBr/EtOH Solutions.** Protonation and complexation experiments show[7,8,23] that interaction with an imine site is stronger than interaction with a nitroxide site for the ligands considered here. In view of this, the very long lifetime of Li-PyNO, three times that of Li-PyIN, is quite unexpected. Comparison between Li-PyNO and Li-PhNO affords another surprise, since protonation of PhNO produces much stronger ESR effects. Nonetheless, a high $^7$Li dipolar relaxation rate in PyNO/LiBr/EtOH, as compared with PhNO, reflects a much longer lived interaction. This is most likely due to strong restraint by transient bond formation between $Li^+$ and the pyridyl nitrogen atom, supplemented by a weaker interaction with the nitroxide oxygen atom. The result is a chelated structure resembling the N,O coordination of $Li^+$ found in $LiCl{\cdot}2Py{\cdot}H_2O$.[18a] Such a chelated structure is favored by closer spacing of bonding sites in PyNO as opposed to PyIN.

In BrPyNO, accessibility of the pyridyl nitrogen site is hindered and the interaction with $Li^+$ is markedly reduced. This is reflected in Table I: both relaxation components $R_d$ and $R_c$, and the calculated sticking time for BrPyNO, lie between PyNO and PhNO or BrPhNO (only monodentate interactions are possible for the latter pair). These results indicate some residual interaction between $Li^+$ and the pyridyl nitrogen coordination site in BrPyNO.

By similar argument, the large dipolar relaxation and underlying $\tau_c$ values for PyIN can best be explained by assuming a weak bidentate complexation of $Li^+$ The small scalar rate for the basic PyIN ligand in comparison with PyNO is due partly to lower peripheral spin density.

**LiCl/MeOH Solutions.** Ligand complexation interactions in LiCl/MeOH contrast sharply with those in LiBr/EtOH. PyNO shows at best a fleeting coordination interaction, and blockage of the pyridyl nitrogen in BrPyNO or its removal in PhNO yields only minor changes in the observed parameters. Errors in the small relaxation rates prevent a more detailed interpretation. For the R-IN ligands, the wide range of enhancement reflects stronger chemical effects in the more polar medium; nonetheless, the low relaxation rate for PyIN indicates overall weaker complexation for R-IN/MeOH systems when compared with R-IN/EtOH.

In previous ESR studies of metal ion complexation with R-IN ligands, we have noted a pronounced solvent effect even for permanently bound adducts.[8] In EtOH, complex formation constants and changes in unpaired spin distribution upon complexation were larger than in $H_2O$, reflecting the weaker solvating power of EtOH. Since solvation of $Li^+$ by MeOH is more exothermic than solvation by EtOH, imidazoline and nitronyl nitroxide ligands should be less competitive as coordination sites in MeOH, in accord with the DNP results.

Proton relaxation rates in the two solvents are in accord with the above argument. By viscosity alone, it would be expected that MeOH rates would be one-third as large as EtOH. In actuality, they are much larger than this, ranging from 0.6 to 1.1 times EtOH rates. The difference between theoretical and observed rates is not large enough to allow assignment of rotational components for MeOH, but the existence of sticking tendencies between MeOH and the radicals is clear. The sticking of MeOH to radical and the expected increased solvation of $Li^+$ together effect a great reduction in radical-$Li^+$ complexation.

**Competitive Complexation.** The nature of the lithium complexes in the present study can be further examined by adding a second metal ion which can compete for radical coordination sites. To test this idea, 1 M $LiNO_3$/MeOH/PyIN was examined with and without $Hg(NO_3)_2$; DNP data are shown in Table II. Without $Hg(NO_3)_2$, $U_{\infty Li}$ is 1000 and the relaxation rates indicate weak $Li^+$ ... PyIN complexation. Addition of $Hg(NO_3)_2$ causes a dramatic decrease in $U_{\infty Li}$ to $-800$ and a decrease in radical-induced relaxation rate $R_{pLi}$ by an order of magnitude. The ESR solution spectra[8] show that $Hg^{2+}$ completely blocks the $\alpha$-diimine coordination site of PyIN by formation of a long-lived, strong Hg-PyIN$^{2+}$ complex ($K_f = 10^4$ l. mol$^{-1}$). It is clear that the very dipolar value of $U_{\infty Li}$, the very small $R_{dLi}$, and the undetectably small $R_{cLi}$ together reflect a complete lack of complexation of $Li^+$ with Hg-PyIN$^{2+}$. The observed $^7$Li DNP data indicate random translational diffusion of $Li^+$ to no closer than $4 \times 10^{-8}$ cm from the cationic complex. The bold Hg effect is a good confirmation of the steric factors invoked earlier to explain enhancement and relaxation in other samples.

**Acknowledgments.** We thank the National Science Foundation (Grant CHE-13760) for partial support of this work, and the NDEA for a fellowship (to J.W.L.).

## References and Notes

(1) (a) Presented in part at the 5th Northeast Regional Meeting of the American Chemical Society, Rochester, N.Y., Oct 1973; see Abstracts, No. 046. (b) Rutgers University; (c) NDEA Predoctoral Fellow, 1969–1972; (d) Georgetown University; (e) ECOM.
(2) K. H. Hausser and D. Stehlik, *Adv. Magn. Reson.*, **3**, 79 (1969).
(3) J. A. Potenza, *Adv. Mol. Relaxation Processes*, **4**, 229 (1972).
(4) E. H. Poindexter, P. J. Caplan, B. E. Wagner, and R. D. Bates, Jr., *J. Chem. Phys.*, **61**, 3821 (1974).
(5) (a) B. E. Wagner, R. D. Bates, Jr., and E. H. Poindexter, *Inorg. Chem.*, **14**, 256 (1975); (b) J. A. Potenza, J. W. Linowski, E. H. Poindexter, B. E. Wagner, and R. D. Bates, Jr., *Mol. Phys.*, **29**, 1597 (1975).
(6) E. F. Ullman, J. H. Osiecki, D. G. B. Boocock, and R. Darcy, *J. Am. Chem. Soc.*, **94**, 7049 (1972).
(7) E. F. Ullman, L. Call, and J. H. Osiecki, *J. Org. Chem.*, **35**, 3623 (1970).
(8) (a) B. E. Wagner, J. N. Helbert, R. D. Bates, Jr., and E. H. Poindexter, *J. Chem. Soc., Chem. Commun.*, 748 (1973); (b) J. N. Helbert, P. W. Kopf, E. H. Poindexter, and B. E. Wagner, *J. Chem. Soc., Dalton Trans.*, 998 (1975).
(9) B. E. Wagner, J. A. Bristol, J. N. Helbert, and E. H. Poindexter, paper presented at the 168th National Meeting of the American Chemical Society, Atlantic City, N.J., Sept 1974, Abstract No. COLL-036.
(10) J. A. Potenza and J. W. Linowski, *J. Chem. Phys.*, **54**, 4095 (1971).
(11) A. Abragam, "The Principles of Nuclear Magnetism", Clarendon Press, Oxford, England, 1961, p 304.
(12) J. E. Wertz and J. R. Bolton, "Electron Spin Resonance: Elementary Theory and Practical Applications", McGraw-Hill, New York, N.Y., 1972, p 199.
(13) E. H. Poindexter, J. R. Stewart, and P. J. Caplan, *J. Chem. Phys.*, **47**, 2862 (1967).
(14) R. D. Bates, Jr., E. H. Poindexter, and B. E. Wagner, *J. Chem. Phys.*, **59**, 3031 (1973).
(15) J. A. D'Anna and J. H. Wharton, *J. Chem. Phys.*, **53**, 4047 (1970).
(16) A. H. Cohen and B. M. Hoffman, *Inorg. Chem.*, **13**, 1484 (1974), and references cited therein.
(17) (a) M. S. Davis, K. Morokuma, and R. W. Kreilick, *J. Am. Chem. Soc.*, **94**, 5588 (1972); (b) J. W. Neely, C. H. Lam, and R. W. Kreilick, *Mol. Phys.*, **29**, 1663 (1975).
(18) (a) F. Durant, P. Piret, and M. Van Meerssche, *Acta Crystallogr.*, **22**, 52 (1967); (b) F. Durant, J. Verbist, and M. Van Meerssche, *Bull. Soc. Chim. Belg.*, **75**, 788 (1966); (c) F. Durant, P. Piret, and M. Van Meerssche, *Acta Crystallogr.*, **23**, 780 (1967).
(19) W. Wong and S. F. Watkins, *J. Chem. Soc., Chem. Commun.*, 888 (1973).
(20) E. Larsen, G. N. LaMar, B. E. Wagner, J. E. Parks, and R. H. Holm, *Inorg. Chem.*, 11, 2652 (1972).
(21) (a) P. Clopath, Ph.D. Thesis, Universitat Freiburg, Switzerland, 1972, Dissertation No. 696; (b) P. Clopath and A. v. Zelewsky, *Helv. Chim. Acta*, **55**, 52 (1972) and references cited therein.
(22) T. Takeshita and N. Hirota, *J. Chem. Phys.*, **58**, 3745 (1973).
(23) C. T. Cazlanis and D. R. Eaton, *Can. J. Chem.*, **52**, 2454 (1974).